

The Gulf of Carpentaria heated Torres Strait and the Northern Great Barrier Reef during the 2016 mass coral bleaching event

Wolanski, E.; Andutta, F.; Deleersnijder, E.; Li, Y.; Thomas, C.J.

DOI

[10.1016/j.ecss.2017.06.018](https://doi.org/10.1016/j.ecss.2017.06.018)

Publication date

2017

Document Version

Accepted author manuscript

Published in

Estuarine, Coastal and Shelf Science

Citation (APA)

Wolanski, E., Andutta, F., Deleersnijder, E., Li, Y., & Thomas, C. J. (2017). The Gulf of Carpentaria heated Torres Strait and the Northern Great Barrier Reef during the 2016 mass coral bleaching event. *Estuarine, Coastal and Shelf Science*, 194, 172-181. <https://doi.org/10.1016/j.ecss.2017.06.018>

Important note

To cite this publication, please use the final published version (if applicable). Please check the document version above.

Copyright

Other than for strictly personal use, it is not permitted to download, forward or distribute the text or part of it, without the consent of the author(s) and/or copyright holder(s), unless the work is under an open content license such as Creative Commons.

Takedown policy

Please contact us and provide details if you believe this document breaches copyrights. We will remove access to the work immediately and investigate your claim.

The Gulf of Carpentaria heated Torres Strait and the Northern Great Barrier Reef during the 2016 mass coral bleaching event

E. Wolanski^{1,*}, F. Andutta^{2,*}, E. Deleersnijder^{3,4,5}, Y. Li^{1,6}, C.J. Thomas^{3,7}

¹ TropWATER and College of Marine & Environmental Sciences, James Cook University, Townsville, Queensland 4811, Australia.

² Griffith Centre for Coastal Management (GCCM), Griffith Climate Change Response Program (GCCRP), and School of Engineering, Griffith University, Gold Coast, Queensland 4222, Australia.

³ Université Catholique de Louvain, Institute of Mechanics, Materials and Civil Engineering (IMMC), B-1348 Louvain-la-Neuve, Belgium.

⁴ Université Catholique de Louvain, Earth and Life Institute (ELI), B-1348 Louvain-la-Neuve, Belgium.

⁵ Delft University of Technology, Delft Institute of Applied Mathematics (DIAM), 2628CD Delft, The Netherlands.

⁶ Yantai Institute of Coastal Zone Research, Chinese Academy of Sciences, Shandong, China.

⁷ Risk Management Solutions, Monument Street, London EC3R 8NB, UK.

* Corresponding author. Email: eric.wolanski@jcu.edu.au

Highlights:

- The Gulf of Carpentaria was an important heat source to Torres Strait and the Northern Great Barrier Reef, in addition to presumably local heating.
- The North Queensland Coastal Current in the Coral Sea ceased, inhibiting cooling of the Northern Great Barrier Reef
- Flushing was slow as is typical of El Nino years and coral bleaching was highest in areas where warm water was trapped.
- The fate of the Great Barrier Reef is controlled by the oceanography of surrounding seas.

The fate of the Great Barrier Reef is controlled by the oceanography of surrounding seas.

Abstract

The 2015/16 ENSO event increased the temperature of waters surrounding northeast Australia to above 30 °C, with large patches of water reaching 32 °C, for over two months, which led to severe bleaching of corals of the Northern Great Barrier Reef (NGBR). This study provides evidence gained from remote-sensing data, oceanographic data and oceanographic modeling, that three factors caused this excessive heating, namely: 1) the shutdown of the North Queensland Coastal Current, which would otherwise have flushed and cooled the Northern Coral Sea and the NGBR through tidal mixing 2) the advection of warm (> 30 °C) water from the Gulf of Carpentaria eastward through Torres Strait and then southward over the NGBR continental shelf, and 3) presumably local solar heating. The eastward flux of this warm water through Torres Strait was driven by a mean sea level difference on either side of the strait that in turn was controlled by the wind, which generated the southward advection of this warm water onto the NGBR shelf. On the NGBR shelf, the residence time of this warm water was longer inshore than offshore, and this may explain the observed cross-shelf gradient of coral bleaching intensity. The fate of the Great Barrier Reef is thus controlled by the oceanography of surrounding seas.

Keywords: Water circulation; heat advection; trapping; stagnation; coral bleaching

Introduction

Coral reefs worldwide, and in the Great Barrier Reef (GBR) in particular, are increasingly degraded by the cumulative impacts of a number of stressors (Douglas, 2003; Hoegh-Guldberg et al., 2007; Brodie and Waterhouse, 2012; Ainsworth et al., 2016), including pollution from terrestrial runoff (Brodie et al., 2012; Fabricius et al., 2016; McCulloch et al., 2003), overfishing (Jackson et al., 2001), predation by crown-of-thorns starfish (Brodie et al., 2005; Fabricius et al., 2010), ocean acidification (Fabricius et al., 2011; Mongin et al., 2016; Golbuu et al., 2016) and increased heat stress (Brown, 1997; Manzello, 2015) that may also promote coral-disease outbreaks and mortality (Precht et al., 2016). Among these stressors, heat stress is the main cause of coral bleaching (Douglas, 2003). Torres Strait (TS) and the northern GBR (NGBR, Figure 1) have long been assumed to be the least likely region of the GBR to be impacted by these stressors because it was healthy and presumed resilient, and because the human impacts from land-use and overfishing have been minimal in the area (Brodie and Pearson, 2016). There were no records of coral bleaching from TS during the anomalously warm years on the GBR (e.g. 1998), but a major bleaching episode apparently occurred for the first time around Thursday Island in 2010 (see location map in Figure 1; Osborne et al., 2013) but the data are too sparse for an assessment of bleaching extent and intensity. Thus the extensive coral bleaching in TS and the NGBR during the 2016 austral summer ENSO event (<http://www.gbrmpa.gov.au/media-room/coral-bleaching>) was an unwelcome surprise (Hughes et al., 2017). In this paper, we propose an oceanographic explanation for what happened. No descriptive analysis of the physical oceanographic aspects of this mass coral bleaching event has been carried out so far. Filling this gap is the objective of the present study. We first describe the domain and summarise what is known of the oceanography of the Northern Coral Sea (NCS), TS and the NGBR. We review the oceanographic, meteorologic and satellite-derived mean sea level and sea surface temperature data for that ENSO event in this area and the surrounding waters of the northern Coral Sea, the Gulf of Papua (GoP) and the Gulf of Carpentaria (GoC). We then use oceanographic models to explain and synthesize these observations. This paper thus reveals the likely sequence of events that led to warm (> 30 °C, peaking at 32 °C) water temperatures over the reefs of NGBR and TS, thereby causing a mass coral bleaching. We also

suggest that the spatial variation of residence time of very warm water over the NGBR shelf explains the observed spatial pattern of coral bleaching. Finally we set the 2016 event within the oceanographic context of previous El Nino episodes.

Site description

The NGBR's lagoon (Figure 1) has limited water exchange with the NCS through a series of narrow reef passages between long reefs that block ~ 80% of the length of the shelf break (Pickard et al., 1977). The water circulation in the NGBR therefore differs from that in the adjoining central GBR region where reefs block only ~ 10 % of the shelf break length, and where, as a result, the South Equatorial Current in the Coral Sea intrudes on the GBR shelf (Wolanski, 1994; Andutta et al., 2013). In the NGBR, the water depth is ~ 10 m on the inner shelf, ~ 30-40 m on the outer shelf, and < 3 m over most reefs (Figure 1). The NGBR has three open boundaries, namely the reef passages linking it with the NCS, the southern boundary across the shelf linking it with the central GBR, and the northern boundary linking it with TS. This southern boundary is largely closed due to a high density of reefs leaving open only a narrow passage (see the arrow in Figure 1c). The net currents over the NGBR are wind-driven, with no evidence of the North Queensland Coastal Current (NQCC), which flows northward offshore from the continental shelf, intruding on the shelf; thus the net currents vanish during calm weather conditions (Wolanski and Ruddick, 1981; Wolanski and Thomson, 1984; Cahill and Middleton, 1993). These net currents are strongly modulated by tidal friction; thus the local tidal currents modulate the net water circulation over the NGBR and the TS (Wolanski and Thomson, 1984).

The TS (Figure 1) connects the GoC to the GoP, the NGBR and the NCS. The bathymetry is extremely complex with numerous islands, reefs, reef passages and shoals. To the west, i.e. on the GoC side of TS, the water depth is ~ 10-20 m. In most of TS the depth varies between 5 and 20 m (Figure 1). Along the eastern boundary of TS, just like on the NGBR, the reefs occupy ~ 80 % of the distance along the shelf break (Pickard et al., 1977). A small, net throughflow occurs through these open boundaries driven by the wind and the mean sea level (MSL) difference across TS (Wolanski et al., 2013).

The NCS is deep (maximum depth in excess of 4000 m) and the surface mixed layer is typically 100 m thick. The net circulation in that layer is driven by the NQCC flowing northward offshore from the NGBR, then veering eastward to flow along the south coast of Papua New Guinea but not intruding over the shallow GoP (Andrews and Clegg, 1989; Wolanski et al., 1995 and 2013; Kessler and Cravatte, 2013). The NQCC thus brings cooler (from higher latitudes) water to the tropical NCS.

Methods

Temperature at depth

The Australian Institute of Marine Science (AIMS) provided time-series data from two temperature loggers deployed at 6.8 m near Thursday Island and 4 m near Woiz Reef in TS (Figure 1). There were no loggers in the NGBR. The hourly data were averaged to generate daily means.

Sea surface temperature (SST) and cloud coverage

Maps of SST were obtained from satellite data based on AVHRR instruments (IMOS, 2016) over the period of 15 Nov 2015 to 1 May 2016. SSTs were extracted on a 2D grid covering the entire NGBR region with a cell size of $0.02^\circ \times 0.02^\circ$, with each cell representing SST averaged over 14 days. SSTs are representative of skin temperature. Whilst the data coverage was limited during cloudy periods, overall they provided a relatively complete picture during most of the time window analysed. We also analysed the 3-day averaged SST data to see if they revealed any additional insights into the dynamics of the warming event; however there was no apparent improvement because of the patchiness of the data due to cloud coverage. Thus we only present the 14-day averaged data here as these were felt to best show the evolution of the warming event. We also examined the cloud images from November 2015 to April 2016 from the Australian Bureau of Meteorology and from the NOAA VIIRS imagery dataset; visually we could not spot any areas with significantly more clouds than the rest, though the data were very patchy in time and space. We also extracted the 14-day averaged SST data at Thursday Island and Woiz Reef from the IMOS (2016) dataset, as well as the data quality level (1: bad; 5: good), for comparison to the AIMS temperature time series at these sites. At Woiz Reef most entries

were acceptable (4) or good (5), but at Thursday Island most were either low (3) or worse (2). Thus we kept only the SST data of quality of least 4 for Woiz Reef and at least 3 for Thursday Island.

Altimetry data

The altimeter MSL data for TS were produced by Ssalto / Duacs and distributed by Aviso, with support from CNES (<http://www.aviso.altimetry.fr/>). The horizontal resolution was 0.25° . These weekly data were used to calculate the difference in the MSL across TS.

Altimetry-derived surface currents in the NCS were obtained from NOAA OSCAR. The spatial and temporal resolution of the data was $1/3^\circ$ and 5 days respectively, from mid-November 2015 to mid-April 2016.

Wind data

The 3-hourly wind data at Coconut Island (a flat island just a few metres above sea level and located ~ 130 km north-east of Cape York, in the southern TS) were obtained from the Australian Bureau of Meteorology. The only other wind data available in TS were those from Horn Island, next to Cape York, but these data were not used in this study because they were aliased by orographic effects (Y. Li, pers. com.).

NCS oceanographic modelling

The drift trajectories in the NCS of warm water plumes originating from the outer GBR were calculated using the method of Oliveira and Stratoudakis (2008) and Wolanski (2016); namely a 2D oceanographic advection-diffusion model was used whereby the advection model was providing to the dispersion model the observed surface currents measured by satellite altimetry. The seeding points were chosen at regular intervals along the western boundary of the NCS fringing the NGBR. A total of 100,000 virtual particles were released in mid-late November 2015. We assumed that the value of the horizontal eddy diffusion coefficient K_x was $10 \text{ m}^2 \text{ s}^{-1}$.

TS and NGBR oceanographic modelling

We could not use altimetry data in TS and the NGBR because the waters are shallow and the currents are strongly influenced by friction and the bathymetry. For TS and the NGBR we used the depth-averaged version of SLIM hydrodynamic model (www.climate.be/slim_flyer). This solves two-dimensional primitive equations on an unstructured mesh. SLIM has already been successfully used to model the circulation in the GBR and TS (Legrand et al., 2006; Lambrechts et al., 2008; Andutta et al., 2012, 2013; Wolanski et al., 2013). Using an unstructured mesh allows the spatial resolution to be made locally higher in shallow areas and near coastlines, where small-scale flow features are important, and lower in deeper areas, where the flow is more uniform. This approach allows the model to resolve a wide range of scales of motion, from regional flows to eddies behind reefs and islands, tidal jets that develop between reefs and islands, as well as intermediate-scale effects such as the sticky waters effect in a dense reef mosaic (Hughes et al., 2008; Andutta et al., 2012). The application of unstructured mesh allows to solve hydrodynamic features of a few tens of meters (Thomas et al., 2014). Much lower resolution models may not reliably solve hydrodynamic processes in such topographically complex areas; such is the case of the SHOC model from eReefs (<http://ereefs.org.au/ereefs>), which has a minimum mesh resolution of >1 km for most reef areas, and also it does not cover the TS and the GoC, rendering it inappropriate for use in this study. The SLIM model domains and the model meshes for TS and NGBR are shown in Figure 1. The TS model forcing follows Wolanski et al. (2013), i.e. it was forced by the tides, the wind at Coconut Island, the MSL data from altimetry, and, along the southern open boundaries, the tidal and the net currents. The tidal currents were taken from Wolanski et al. (2013). According to the historical field measurements of Wolanski and Ruddick (1981), Wolanski and Thomson (1984) and Cahill and Middleton (1993) for the NGBR and from Wolanski (1993) for the GoC, the net currents were proportional to the wind and vanished in calm weather conditions. The coefficient of proportionality between winds and net currents was derived from these historical field data. Forcing by wave breaking on the reef crest at the

shelf break was assumed to be negligible because (see later) the dominant wind was seaward and wind waves and swell are negligible in this area under such wind conditions in the absence of storms or cyclones elsewhere in the Coral Sea (EW, unpublished). The NGBR model was similarly forced by the wind at Coconut Island as no other data were available, the tides in the NCS, and the tidal and net currents over the southern and northern open boundaries over the NGBR shelf. To follow the trajectories of warm water plumes, we released particles at a number of points and we followed their trajectories. River discharges were negligible in the 2016 austral summer, and thus were not included in the simulations.

Results

Figure 2 shows time-series plot of the satellite-derived 14-day average SST and the observed water temperature at depth recorded by the AIMS temperature loggers at Thursday Island and Woiz Reef. The two data sets agree well with each other. The data show heating by 2°C from mid-December 2015 to a temperature peak on 1 February 2016, followed by a slight cooling, and then a rapid heating with the temperature reaching ~ 32 °C and 31 °C at Thursday Island and Woiz Reef respectively by around 11 March 2016. Stepwise cooling occurred afterward.

Figure 3 shows sequential plots of the distribution of SST in the NGBR, TS and surrounding waters. On December 12, 2015, warm water was present only in the southern portion of the eastern GoC. On December 26, 2015, warm water (> 30 °C) had occurred in both the southern and northern regions of the GoC. By January 9, 2016, warm water had spread in the northern and southern TS and over coastal waters of the GoP, and Princess Charlotte Bay was also heating in isolation. By January 23, the GoC was measurably heated and a warm water plume occurred from the southern TS into the far northern region of the NGBR. This warm water plume spread southward and covered much of the NGBR by February 6, 2016. By February 20, 2016, this water had become even warmer, reaching 32°C in the central region of the NGBR. On February 27 the temperature in most of the far-northern NGBR and the whole of TS exceeded 30 °C, with patches reaching and sometimes exceeding 32 °C. Throughout March the SST data in the NGBR were very patchy. For instance in the SST image for March 19, 2016 (Figure 3h) there are very few pixels in the northern NGBR, meaning there was little

data available there, likely due to cloud cover. On April 2, 2016, the temperature in most of the NGBR and TS waters was $> 30\text{ }^{\circ}\text{C}$, with small patches at $32\text{ }^{\circ}\text{C}$. The SST was measurably cooler by April 9, 2016 and the temperature in most of the NGBR and the southern TS was at $28\text{ }^{\circ}\text{C}$ by April 16, 2016, though the far northern TS and the GoC still remained warm ($\sim 30\text{ }^{\circ}\text{C}$).

It is only by the end of February 2016 that warm water pools occurred in the NCS, but there is no evidence of this warm water intruding in the NGBR or TS. Instead there seems to exist a thin layer of cooler water along the outer NGBR shelf separating these waters. Figure 3 also shows cooler water filaments along the shelf break.

Figure 4 shows sequential plots of the altimetry-derived surface currents in the GoP and the NCS. Altimetry measured a net eastward flow through TS from December 2015 to March 2016, however the strength of these currents was likely to have been greatly overestimated because these data neglect the high friction in shallow waters. There was no NQCC in December 2015; it reformed but was very weak (speed $< 0.07\text{ m s}^{-1}$) in January and February 2016 and it disappeared again in March and reformed in April 2016. From January to March 2016, there was a counter-clockwise circulation in the northern NCS and the GoP, as well as a southward flow in the NCS along the shelf break of the NGBR.

Figure 5 shows the predicted fate from November 2015 to February 2016 of virtual particles released in the NCS along the shelf break of the NGBR, using the NCS oceanographic model based on altimetry current data. The particles were initially exported seaward south-eastward, then advected northeastward across the NCS, and finally they moved southwestward across the NCS again to return near the original seeding sites after four months.

The dominant wind was south-eastward occurring in three events during the 2016 austral summer while the wind speed was generally $< 8\text{ m s}^{-1}$ (Figure 6). The wind generated a uniform MSL difference across TS of up to 0.8 m (Figure 6), the western side (GoC) being higher than the eastern side (GoP and NCS), and the MSL difference increased with increasing wind speed and vanished during calm weather (Figure 6). The MSL varied slightly in the NCS.

Figure 7 shows the predicted trajectories over 20 days of virtual Lagrangian particles seeded in the TS domain on February 1, 2016, using the SLIM model. The particles moved eastward from the

GoC into TS after 5 days. After crossing the passages in the western TS, some of these particles, as well as the particles seeded in TS itself, moved northeastward while the majority of the particles moved southward into the NGBR on the inner shelf. The flow took approximately three weeks to flow through TS and enter the NGBR, during which time a large dispersion occurred.

Figure 8 shows the predicted trajectories over 45 days in February-March 2016 of virtual warm water Lagrangian particles seeded on the inner shelf of the northern NGBR domain on February 1, 2016, following the predictions (Figure 7) of the intrusion zone of the warm water plume from the GoC. The warm water particles moved southward longshore but did not reach Princess Charlotte Bay. Instead the majority progressively dispersed cross-shelf; on reaching the outer shelf they were rapidly (in a few days) flushed into the NCS by the strong tidal currents in that area due to the tidal jets forming in reef passages. About 30% of the particles were trapped in the mid-shelf reef mosaic and in shallow, coastal embayments.

Discussion

The good fit between SST and temperature at depth suggests that the waters were vertically well-mixed in this shallow domain, justifying the use of a 2D hydrodynamic model.

The satellite-measured SST showed that the 2016 ENSO heating started in the Gulf of Carpentaria (GoC). The SST data also suggest that this warm ($> 30\text{ }^{\circ}\text{C}$) GoC water entered the Torres Strait (TS) through passages at its southern side and then slowly spread both southward on the inner shelf into the Northern Great Barrier Reef (NGBR) and also northward towards the northern TS. This is supported by the wind data (Figure 6), which show consistent westerly winds in TS during this period. An extremely warm water ($\sim 32\text{ }^{\circ}\text{C}$) pool formed on the inner and mid-shelf of the NGBR, in an area of high reef density. The NCS also heated, but much less and a thin streak of colder water occurred all along the reefs at the shelf break. We suspect this cold water streak was due to vertical mixing of deep, cold oceanic water upwelled by tidal jets in reef passages (Thomson and Wolanski 1984; Wolanski et al. 1988).

Altimetry-derived surface currents suggest that the North Queensland Coastal Current, which would normally flush and cool the NCS and, by tidal mixing, the outer shelf of the NGBR, actually did the opposite, namely it reversed sign and brought warm water from the TS and the Gulf of Papua (GoP) to the NCS along the NGBR. A simple 2D advection-diffusion model based on these observed currents suggests that a counter-clockwise circulation occurred in the NCS and the GoP during this ENSO event and that this trapped warm water in the NCS.

Oceanographic modeling using the tides, the local wind and the satellite-derived mean sea level difference across Torres Strait reproduced qualitatively well the observations of GoC warm water plume intrusion in the TS, and suggests the likely mechanism: consistent westerly winds set up a mean sea level gradient across TS (Figure 6), which in turn, together with the wind, set up a net eastward current through TS, transporting the warm water plume from GoC across TS and into the northern NGBR (Figure 6). The modelling also shows that this plume split into a plume moving northward on the outer shelf towards the northeast region of TS and another plume moving southward in the NGBR on the inner shelf. On reaching the southern third of the NGBR, the plume mixed cross-shelf. On reaching the outer shelf the warm water was rapidly (in a few days) flushed into the NCS by the strong tidal currents in that area due to the tidal jets forming in reef passages. About 30% of the particles were trapped in the mid-shelf reef mosaic as a result of the sticky water effect (Andutta et al. 2012) and in shallow, coastal embayments. The location of this predicted stagnation area (Figure 8) corresponds qualitatively well with the SST data in the NGBR (Figure 3). Similarly the model reproduced qualitatively well the observations from the SST data that the very warm water plumes were largely restricted to the inner and mid-shelf.

Figure 9 shows the map of bleaching intensity of corals in the NGBR. It shows smaller bleaching on the outer shelf than on the inner and mid-shelf. Because bleaching is a function of both the temperature and the residence time of that warm water over the coral reefs, our oceanographic findings that the residence time of warm water was smaller offshore than inshore qualitatively explains the bleaching map. The large patch of largely not-bleached corals on the mid-shelf in the NCS just south of Torres Strait may be explained by the modeling predictions that the intrusive GoC warm water plume was confined to the inner shelf in this area of the NGBR. The southwest to

northeast streaks of coral bleaching in the southern Torres Strait (Figure 9) also appear to be explained by the oceanography, as our study suggests (Figures 7 and 8) that the intruding GoC warm water split in two plumes, one plume spreading north-eastward in TS and the other plume spreading southward along the mid- and inner shelf of the NGBR.

It should be noted that this study is to some extent subjective due to the lack of oceanographic field data available for the 2016 ENSO event for verifying the models. What we presented is our best-informed attempt to reveal the mechanisms involved in causing the event, based on the available data combined with existing body of knowledge of the water circulation in and around the TS/NGBR region. The models employed here have previously been used extensively to study water flow in the region, and are forced and calibrated with real oceanographic data at the open boundaries. Likewise, the lack of oceanographic dispersion data means it is not possible to derive a precise value for the horizontal eddy diffusivity parameter K_x , so the value used was estimated to be $10 \text{ m}^2 \text{ s}^{-1}$ from Wolanski and Elliott (2015). A smaller (larger) value of K_x would result in smaller (higher) dilution of the warm water plume. Finally, we do not propose a heat budget to quantify how much additional heating was due to local solar heating. We do demonstrate that oceanographic advection of warm water from the Gulf of Carpentaria played a significant contributory role in the 2016 ENSO event.

What was so special about the 2016 ENSO event that the corals in TS were extensively bleached? The eastward net flow through Torres Strait during the austral summer is generated by the southeastward monsoonal wind, this generates a wind stress as well as a difference of the mean sea level (ΔMSL) across Torres Strait (Figure 6). Figure 10 reveals that the seasonally-averaged mean sea level difference across Torres Strait $\langle\Delta\text{MSL}\rangle$ (i.e. averaged from 1 January to 31 March) varied interannually and was highly correlated ($r^2 = 0.71$) with the seasonally-averaged Southern Oscillation Index ($\langle\text{SOI}\rangle$). El Nino events correspond to the smallest $\langle\Delta\text{MSL}\rangle$ and $\langle\text{SOI}\rangle$. A negative $\langle\text{SOI}\rangle$ is correlated with increased summer temperature in the NGBR/TS region, due to lower cloud cover (Osborne et al., 2013; BOM, 2017). From Figure 10, an eastward flow prevailed in the austral summer in all years since 1993. However the intensity of that flow varied interannually. A negative $\langle\text{SOI}\rangle$ is correlated with small $\langle\Delta\text{MSL}\rangle$, and thus with higher water residence time in TS. So during El Nino

years, the lower cloud cover and warmer atmosphere more effectively heats up the shallow waters of the Gulf of Carpentaria and TS and these waters reside for longer than normal due to the small $\langle \Delta \text{MSL} \rangle$. We hypothesise that this is the primary mechanism for bleaching in TS, and potentially also in the northern NGBR. When the input waters from GoC are also warm however, then this further facilitates the process. Thus we suggest that 2016 was the perfect storm of these factors that lead to mass coral bleaching. We also suggest that differential heating of Gulf of Carpentaria waters from year to year may explain the TS coral bleaching in 2016 and not in 1998 when $|\langle \text{SOI} \rangle|$ was larger, and this may also explain the massive die-offs of mangroves in the Gulf of Carpentaria in 2016 and not in 1998 (N. Duke, pers. com.; <https://research.jcu.edu.au/tropwater/news-and-events/large-scale-mangrove-dieback-unprecedented>).

List of acronyms

AIMS	Australian Institute of Marine Science
AVHRR	Advanced Very High Resolution Radiometer
ENSO	El Nino - Southern Oscillation
GBR	Great Barrier Reef
GoC	Gulf of Carpentaria
GoP	Gulf of Papua
MSL	mean sea level
NCS	Northern Coral Sea
NGBR	Northern Great Barrier Reef
NQCC	North Queensland Coastal Current
SOI	Southern Oscillation Index
SST	sea surface temperature
TS	Torres Strait

References

- Ainsworth, T.D., Heron, S.F., Ortiz, J.C., Mumby, P.J., Grech, A., Ogawa, D., Eakin, C.M., Leggat, W., 2016. Climate change disables coral bleaching protection on the Great Barrier Reef. *Science* 352, 338-342.
- Andrews, J.C., Clegg, S., 1989. Coral Sea circulation deduced from modal information models. *Deep Sea Research* 36, 957-974.
- Andutta, F., Kingsford, M., Wolanski, E., 2012. 'Sticky water' enables the retention of larvae in a reef mosaic. *Estuarine, Coastal and Shelf Science* 101, 54-63.
- Andutta, F., Ridd, P.V., Wolanski, E., 2013. The age and the flushing time of the Great Barrier Reef waters. *Continental Shelf Research* 53, 11-19.
- BOM (Bureau of Meteorology), 2017. <http://www.bom.gov.au/climate/enso/history/ln-2010-12/ENSO-temperature.shtml>
- Brodie, J., Waterhouse, J., 2012. A critical assessment of environmental management of the 'not so Great' Barrier Reef. *Estuarine, Coastal and Shelf Science* 104-105, 1-22.
- Brodie, J., Pearson, R.G., 2016. Ecosystem health of the Great Barrier Reef: Time for effective management action based on evidence. *Estuarine, Coastal and Shelf Science* 183, 438-451.
- Brodie, J., Fabricius, K., De'ath, G., Okaji, K., 2005. Are increased nutrient inputs responsible for more outbreaks of crown-of-thorns starfish? An appraisal of the evidence. *Marine Pollution Bulletin* 51, 266-278.
- Brodie, J.E., Kroon, F.J., Schaffelke, B., Wolanski, E., Lewis, S., Devlin, M.J., Bohnet, I., Bainbridge, Z.T., Waterhouse, J., Davis, A.M., 2012. Terrestrial pollutant runoff to the Great Barrier Reef: an update of issues, priorities and management responses. *Marine Pollution Bulletin* 65, 81-100.
- Brown, B.E., 1997. Coral bleaching: causes and consequences. *Coral Reefs* 16, 129-138.
- Cahill, M.L., Middleton, J.H., 1993. Wind-forced motion on the northern Great Barrier Reef. *Journal of Physical Oceanography* 23, 1176-1191.
- Douglas, A.E., 2003. Coral bleaching—how and why? *Marine Pollution Bulletin* 46, 385–392.

- Fabricius, K.E., Okaji, K., De'ath, G., 2010. Three lines of evidence to link outbreaks of the crown-of-thorns seastar *Acanthaster planci* to the release of larval food limitation. *Coral Reefs* 29 (3), 593-605.
- Fabricius, K.E., Langdon, C., Uthicke, S., Humphrey, C., Noonan, S., De'ath, G., Okazaki, R., Muehllehner, N., Glas, M.S., Lough, J.M., 2011. Losers and winners in coral reefs acclimatized to elevated carbon dioxide concentrations. *Nature Climate Change* 1, 165–169.
- Fabricius, K.E., Logan, M., Weeks, S.J., Lewis, S.E., Brodie, J., 2016. Changes in water clarity related to river discharges on the Great Barrier Reef continental shelf: 2002-2013. *Estuarine, Coastal and Shelf Science* 173, A1-A15.
- Golbuu, Y., Gouezo, M., Kurihara, H., Rehm, L., Wolanski, E., 2016. Long-term isolation and local adaptation in Palau's Nikko Bay help corals thrive in acidic waters. *Coral Reefs* 35, 909-918.
- Hoegh-Guldberg, O., Mumby, P.J., Hooten, A.J., Steneck, R.S., Harvell, C.D., Sale, P.F., Caldeira, K., Knowlton, N., Eakin, C.M., Iglesias-Prieto, R., Muthiga, N., Bradbury, R.H., Dubi, A., Hatzioios, M.A., 2007. Coral reefs under rapid climate change and ocean acidification. *Science* 318, 1737–1742.
- Hughes, M.G., Harris, P.T., Heap, A., Hemer, M.A., 2008. Form drag is a major component of bed shear stress associated with tidal flow in the vicinity of an isolated sand bank, Torres Strait, northern Australia. *Continental Shelf Research* 28, 2203-2213.
- Hughes, T.P., Kerry, J.T., Alvares-Noriega, M., et al., 2017. Global warming and recurrent mass bleaching of corals. *Nature* 543, 373-377.
- Jackson, J.B.C., Kirby, M.X., Berger, W.H., Bjorndal, K.A., Botsford, L.V., Bourque, B.J., Bradbury, R.H., Cooke, R., Erlandson, J., Estes, J.A., Hughes, T.P., Kidwell, S., Lange, C.B., Lenihan, H.S., Pandolfi, J.M., Peterson, C.H., Steneck, R.S., Tegner, M.J., Warner, R.R., 2001. Historical overfishing and the recent collapse of coastal ecosystems. *Science* 293, 629-638.
- Krishna Rao, P., Smith, W.L., Koffler, R., 1972. Global sea-surface temperature distribution determined from an environmental satellite. *Monthly Weather Review* 10, 10-14.

- Lambrechts, J., Hanert, E., Deleersnijder, E., Bernard, P.-E., Legat, V., Remacle, J.-F., Wolanski, E., 2008. A multi-scale model of the hydrodynamics of the whole Great Barrier Reef. *Estuarine, Coastal and Shelf Science* 79, 143–151.
- Legrand, S., Deleersnijder, E., Hanert, E., Legat, V., Wolanski, E., 2006. High-resolution, unstructured meshes for hydrodynamic models of the Great Barrier Reef, Australia. *Estuarine, Coastal and Shelf Science* 68, 36-46.
- Manzello, D.P., 2015. Rapid recent warming of coral reefs in the Florida Keys. *Nature Scientific Reports* 5:16762, doi: 10.1038/srep16762.
- Mongin, M., Baird, M.E., Tilbrook, B., Matear, R.J., Lenton, A., Herzfeld, M., Wild-Allen, K., Skerratt, J., Margvelashvili, N., Robson, B.J., Duarte, C.M., Gustafsson, M.S.M., Ralph, P.J., Steven, A.D.L., 2016. The exposure of the Great Barrier Reef to ocean acidification. *Nature Communications* 7:10732.
- Oliveira, P.B., Stratoudakis, Y., 2008. Satellite-derived conditions and advection patterns off Iberia and NW Africa: potential implications to sardine recruitment dynamics and population structuring. *Remote Sensing Environment* 112, 3376-3387.
- Osborne, K., Miller, I., Johns, K., Jonker, M., Sweatman, H., 2013. Preliminary report on surveys of biodiversity of fishes and corals in Torres Strait. Report to the National Environmental Research Program. Reef and Rainforest Research Centre Limited, Cairns, 33 pp.
- Pickard, G.L., Donguy, J.R., Henin, C., Rougerie, F., 1977. A review of the physical oceanography of the Great Barrier Reef and western Coral Sea. Australian Institute of Marine Sciences, Monography Series vol. 2 Australian Government Printer, Canberra, 134 pp.
- Precht, W.F., Gintert, B.E., Robbart, M.L., Fura, R., van Woesik, R., 2016. Unprecedented disease-related coral mortality in Southeastern Florida. *Nature Scientific Reports* 6:31374, doi: 10.1038/srep31374.
- Thomas, C.J., Lambrechts, J., Wolanski, E., Traag, V.A., Blondel, V.D., Deleersnijder, E., Hanert, E., 2014. Numerical modelling and graph theory tools to study ecological connectivity in the Great Barrier Reef, *Ecological Modelling* 272, 160-174.

- Thomson, R.E., Wolanski, E., 1984. Tidal period upwelling within Raine Island Entrance, Great Barrier Reef. *Journal of Marine Research* 42, 787-808.
- Wolanski, E., 1993. Water circulation in the Gulf of Carpentaria. *Journal of Marine Systems* 4, 401-420.
- Wolanski, E., 1994. *Physical oceanography processes of the Great Barrier Reef*. CRC Press, Boca Raton, Florida, 194 pp.
- Wolanski, E., Ruddick, B., 1981. Water circulation and shelf waves in the northern Great Barrier Reef lagoon. *Australian Journal Marine Freshwater Research* 32, 721-740.
- Wolanski, E., Pickard, G.L., Jupp, D.L.B., 1984. River plumes, coral reefs and mixing in the Gulf of Papua and the northern Great Barrier Reef. *Estuarine Coastal and Shelf Science* 18, 291-314.
- Wolanski, E., Thomson, R.E., 1984. Wind-driven circulation on the northern Great Barrier Reef continental shelf in summer. *Estuarine, Coastal and Shelf Science* 18, 271-289.
- Wolanski, E., Drew, E., Abel, K., O'Brien, J., 1988. Tidal jets, nutrient upwelling and their influence on the productivity of the algal *Halimeda* in the Ribbon Reefs, Great Barrier Reef. *Estuarine, Coastal and Shelf Science* 26, 169-201.
- Wolanski, E., Norro, A., King, B., 1995. Water circulation in the Gulf of Papua. *Continental Shelf Research* 15, 185-212.
- Wolanski, E., Elliott, M., 2015. *Estuarine Ecohydrology. An Introduction*. Elsevier, Amsterdam. 322 pp.
- Wolanski, E., 2016. Bounded and unbounded boundaries – Untangling mechanisms for estuarine-marine ecological connectivity: Scales of m to 10,000 km – A review. *Estuarine, Coastal and Shelf Science*. <http://dx.doi.org/10.1016/j.ecss.2016.06.022>.

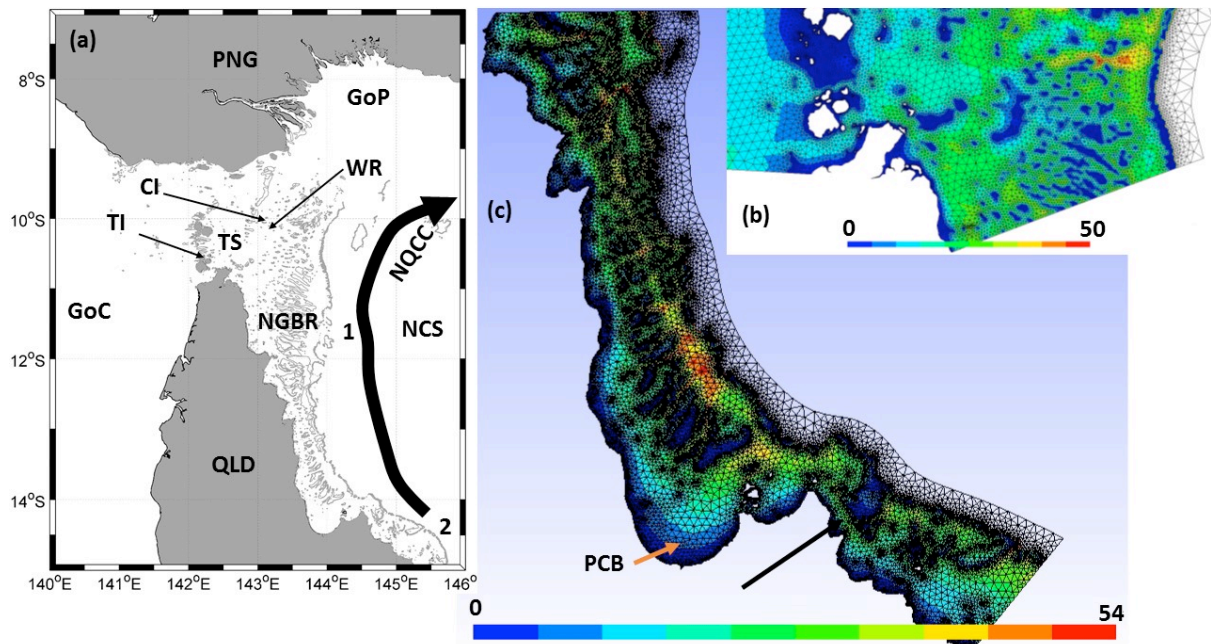


Figure 1: (a) General location map showing the Gulf of Carpentaria (GoC), Torres Strait (TS), Northern Great Barrier Reef (NGBR), Northern Coral Sea (NCS), Gulf of Papua (GoP), Queensland (QLD), Papua New Guinea (PNG) and the North Queensland Coastal Current (NQCC). (b) Zoom-in of the southern region of the TS model domain, showing the mesh and the bathymetry (depth in m). (c) The NGBR model domain showing the mesh and the bathymetry (depth in m). The thick black arrow in (c) points to the shallow, narrow channel connecting the NGBR with the remaining Great Barrier Reef further south. PCB=Princess Charlotte Bay. TI: Thursday Island; CI: Coconut Island; WR: Woiz Reef; 1 and 2 are location points in the NCS where Mean Sea Level data were obtained from altimetry.

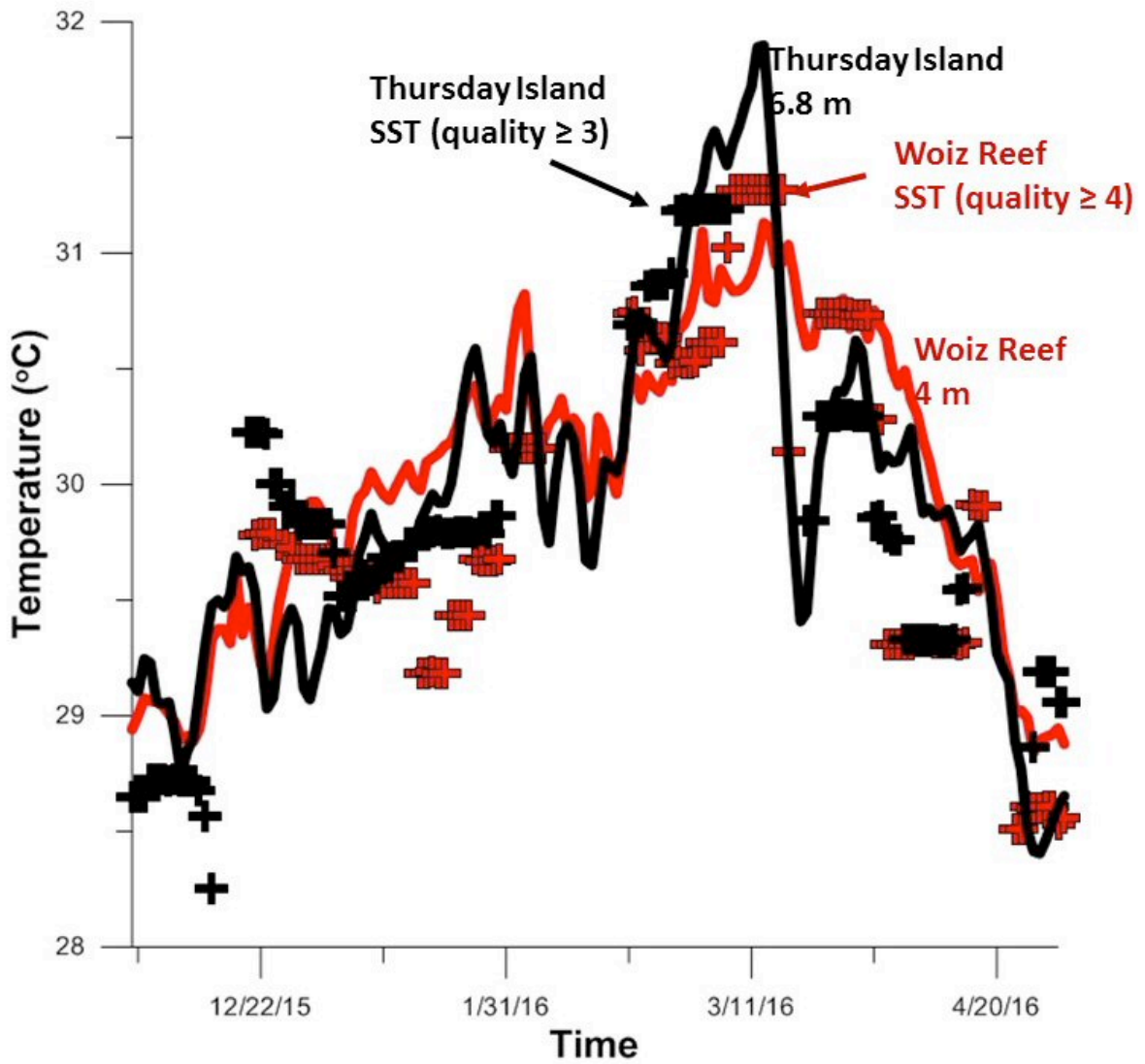


Figure 2: Time-series plot of (—) the daily averaged temperature at depth and (+) the 14-days averaged satellite-derived SST at Thursday Island and Woiz Reef.

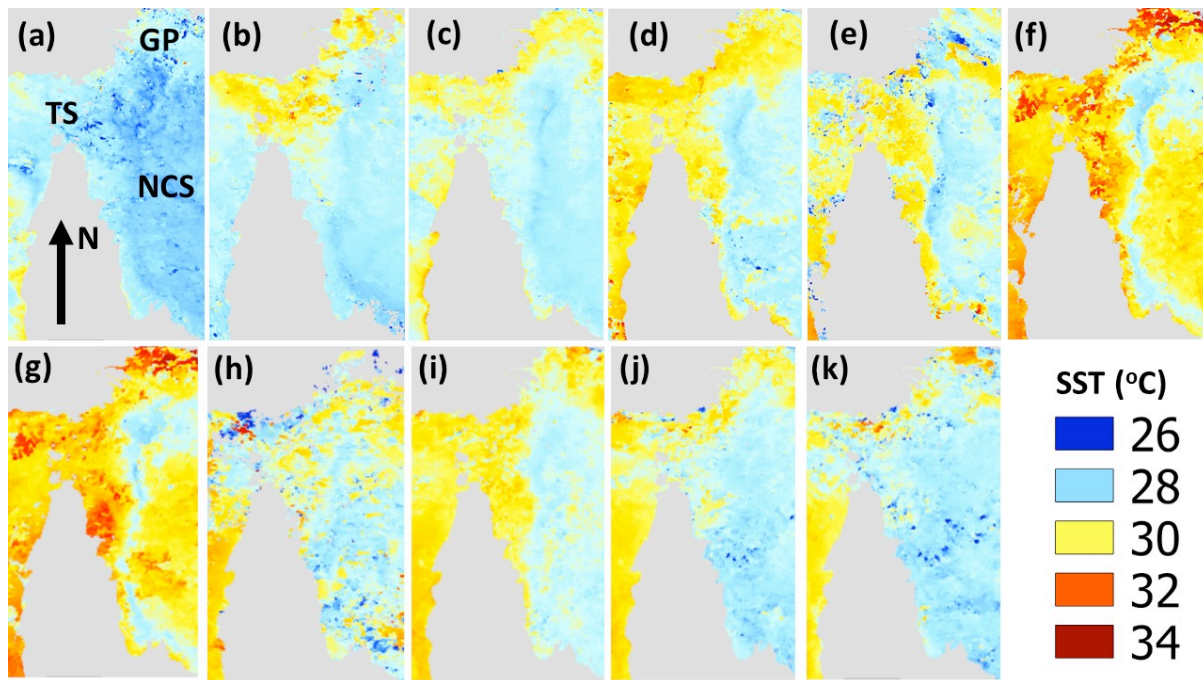


Figure 3: Observed SST between December-2015 and March 2016 (source: <https://help.aodn.org.au/satellite-data/product-information/>). (a) December 12, 2015; (b) December 26, 2015; (c) January 9, 2016; (d) January 23, 2016; (e) February 6, 2016; (f) February 20, 2016; (g) February 27, 2016; (h) March 19, 2016; (i) April 2, 2016; (j) April 9, 2016; (k) April 16, 2016.

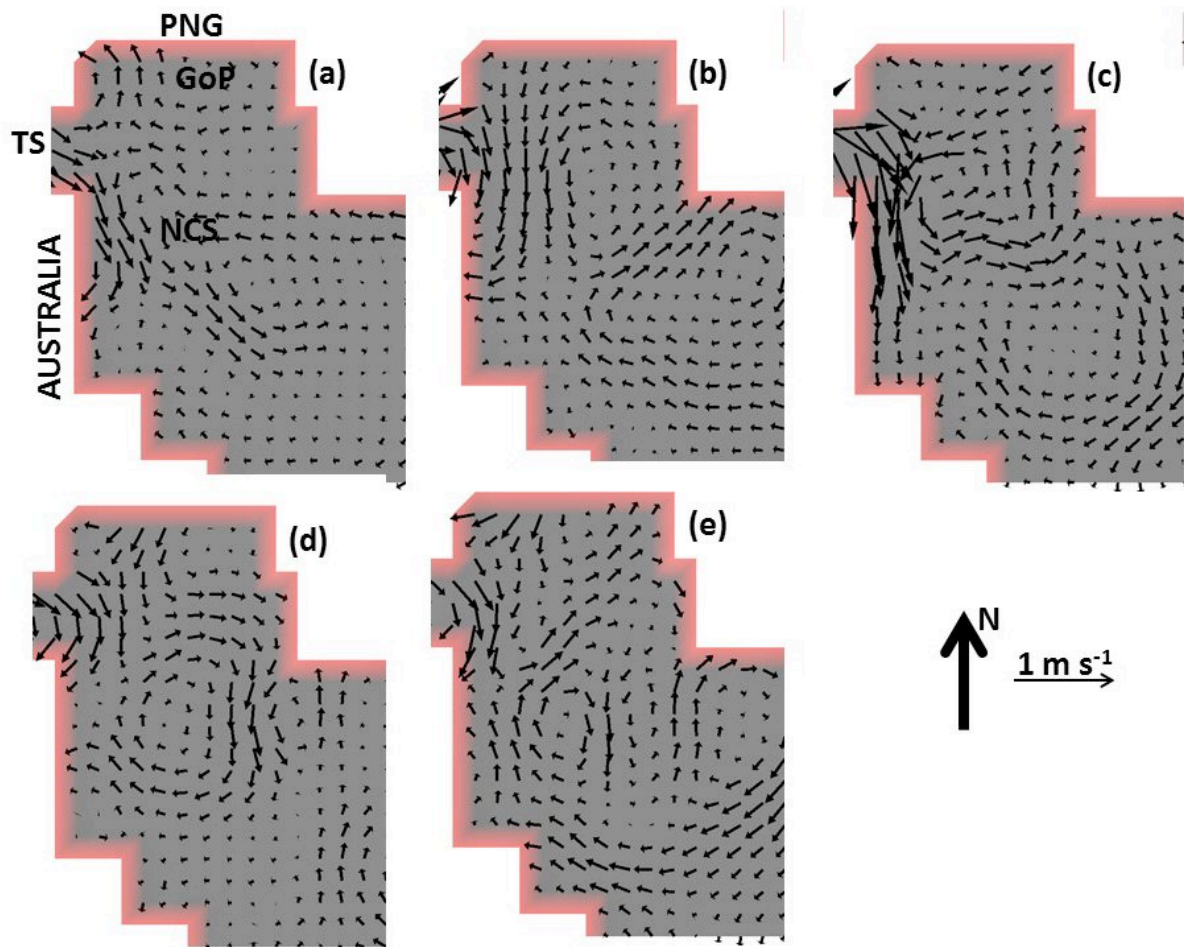


Figure 4: Altimetry-derived, 5-days averaged, surface currents in the NCS on (a) December 15, 2015, (b) January 15, 2016, (c) February 15, 2016, (d) March 15, 2016 and (e) April 15, 2016. TS=Torres Strait, PNG=Papua New Guinea, GoP=Gulf of Papua, NCS=Northern Coral Sea.

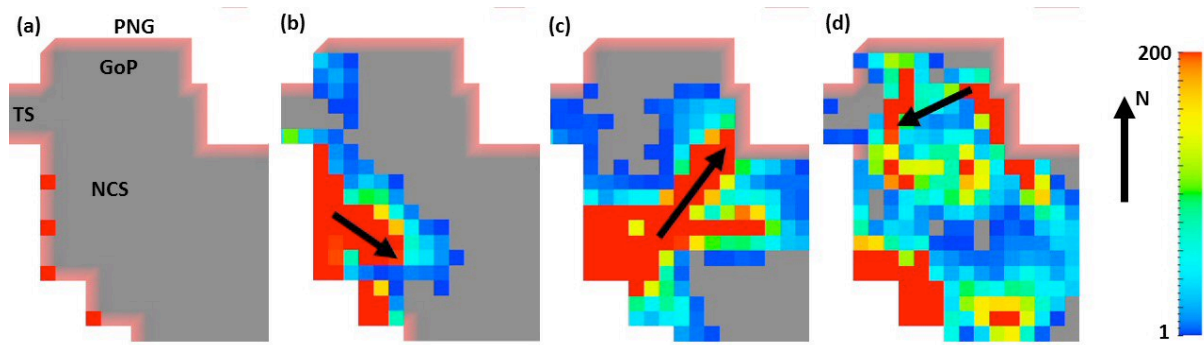


Figure 5: Using the altimetry-derived currents, snapshots of the predicted particle plume in the Northern Coral Sea (NCS) and the Gulf of Papua (GoP) on (a) November 20, 2015 (this shows the assumed seeding sources in the NCS at the continental shelf break of the NGBR), (b) December 20, 2015, (c) January 20, 2016 and (d) February 20, 2016. The arrows indicate the general movement of the particles. The colour bar shows the number of particles per cell.

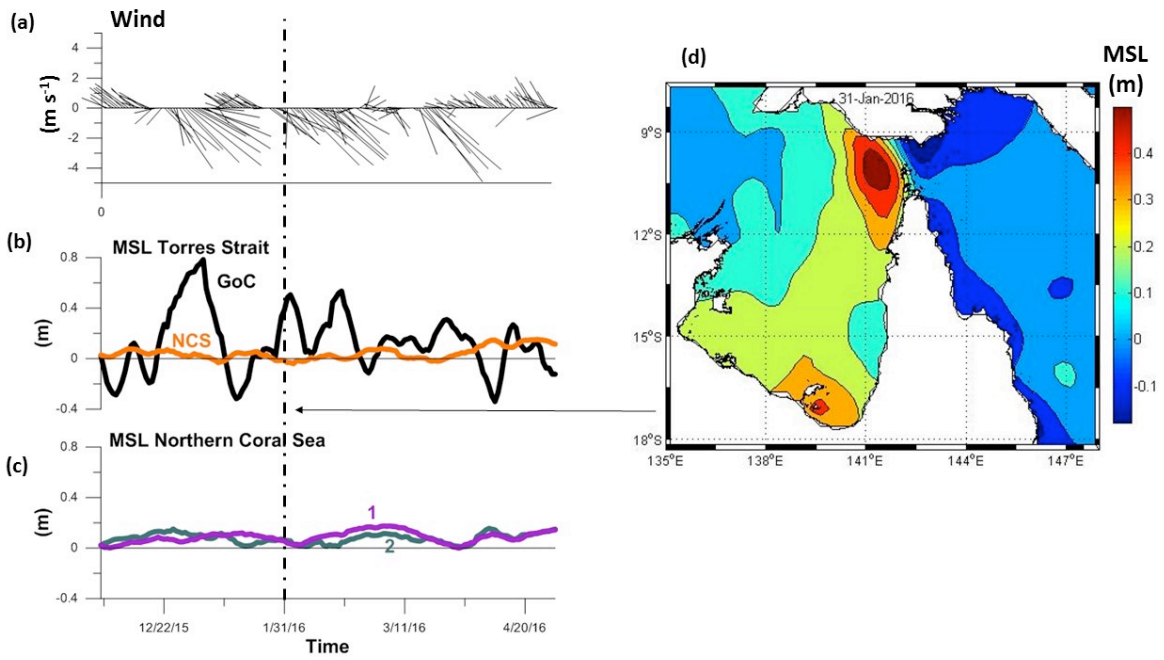


Figure 6: (Left) Time-series plot during the 2016 austral summer of (a) the wind vectors at Coconut Island, (b) the altimetry-measured Mean Sea Level (MSL) at the eastern (NCS) and western (GoC) open boundaries of the Torres Strait model domain shown in Figure 1, and (c) the MSL in the Coral Sea at sites 1 and 2 shown in Figure 1. The vertical dashed line indicates January 31, 2016. (d) Spatial distribution of the MSL on January 31, 2016.

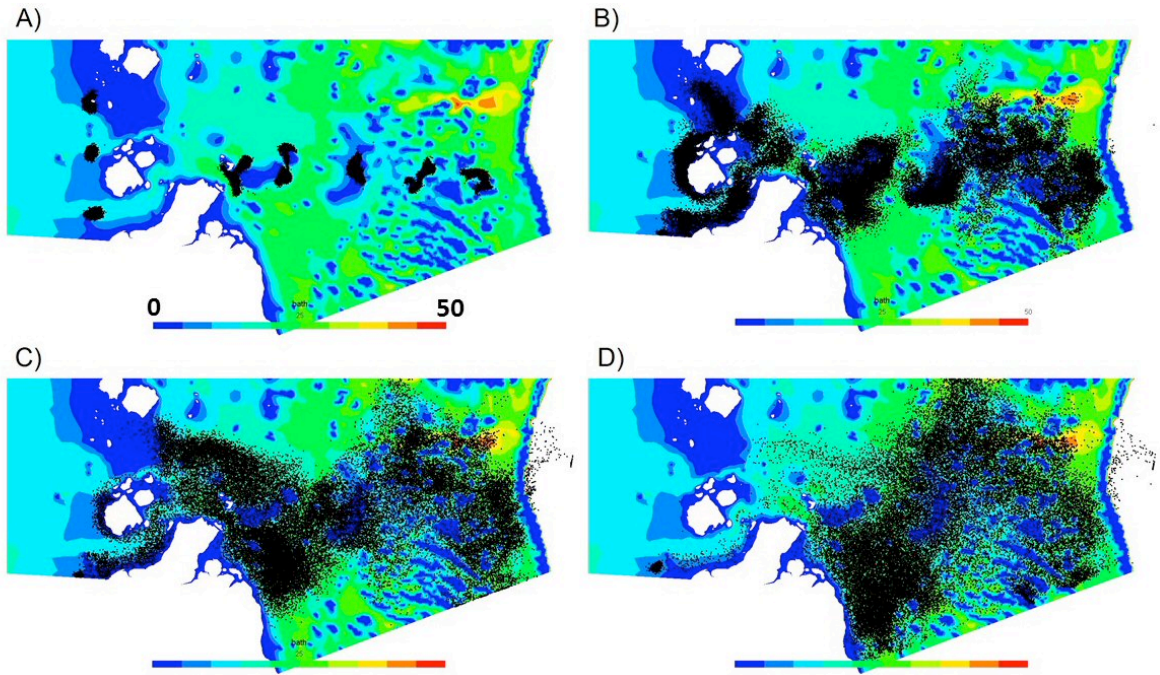


Figure 7: SLIM-model predictions of the plumes of virtual warm water particles at midnight on (A) February 1, 2016, (B) February 5, (C) February 10, and (D) February 20. The particles were released at 0 h on February 1. The colour bar shows the depth (in m).

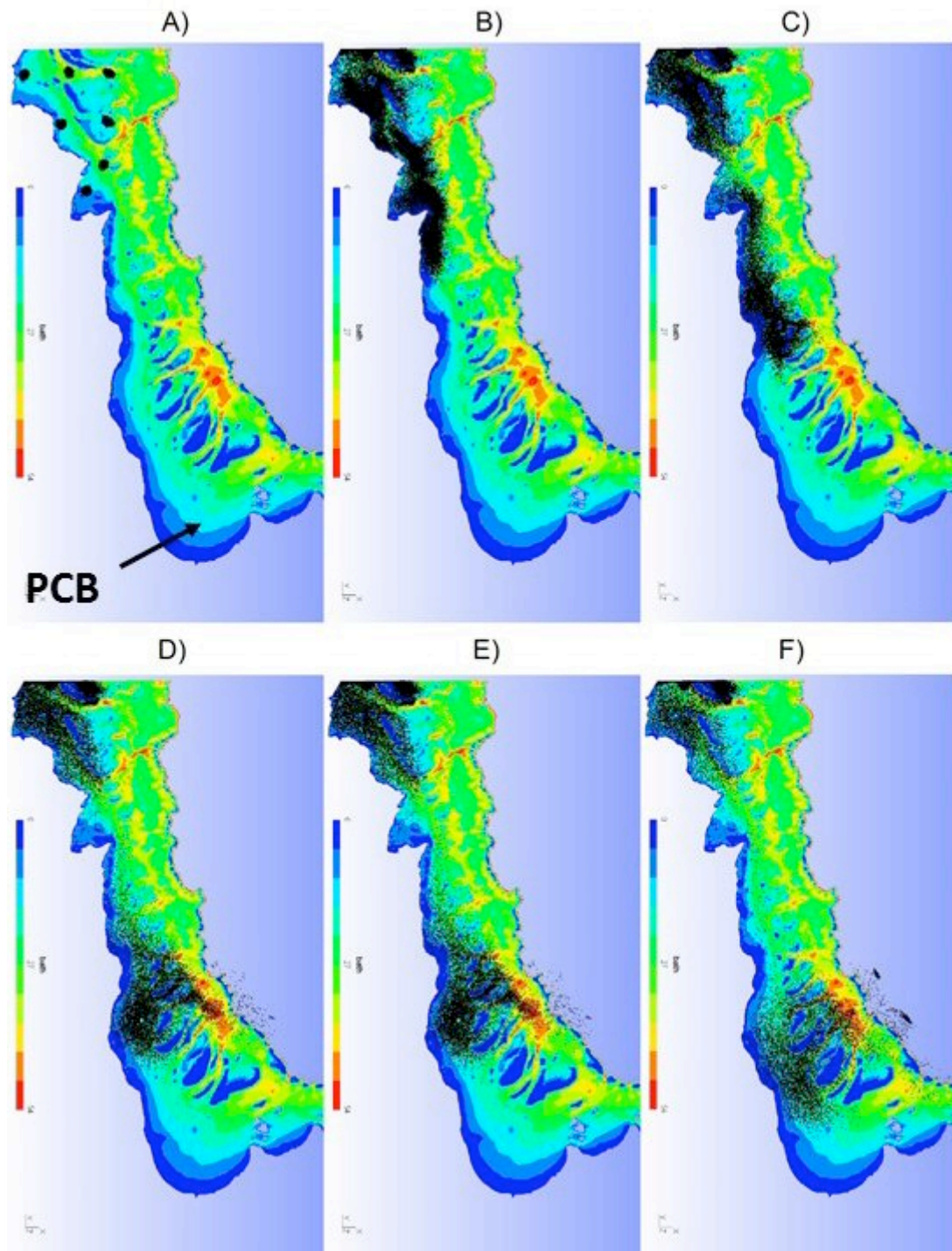


Figure 8: SLIM-model predictions of the plumes of virtual warm water particles on (A) February 1, 2016 (24 hours after their release in the NGBR), and (B-F) after 10, 20, 30, 40 and 45 days, respectively. PCB=Princess Charlotte Bay. The colour bar shows the depth (in m).

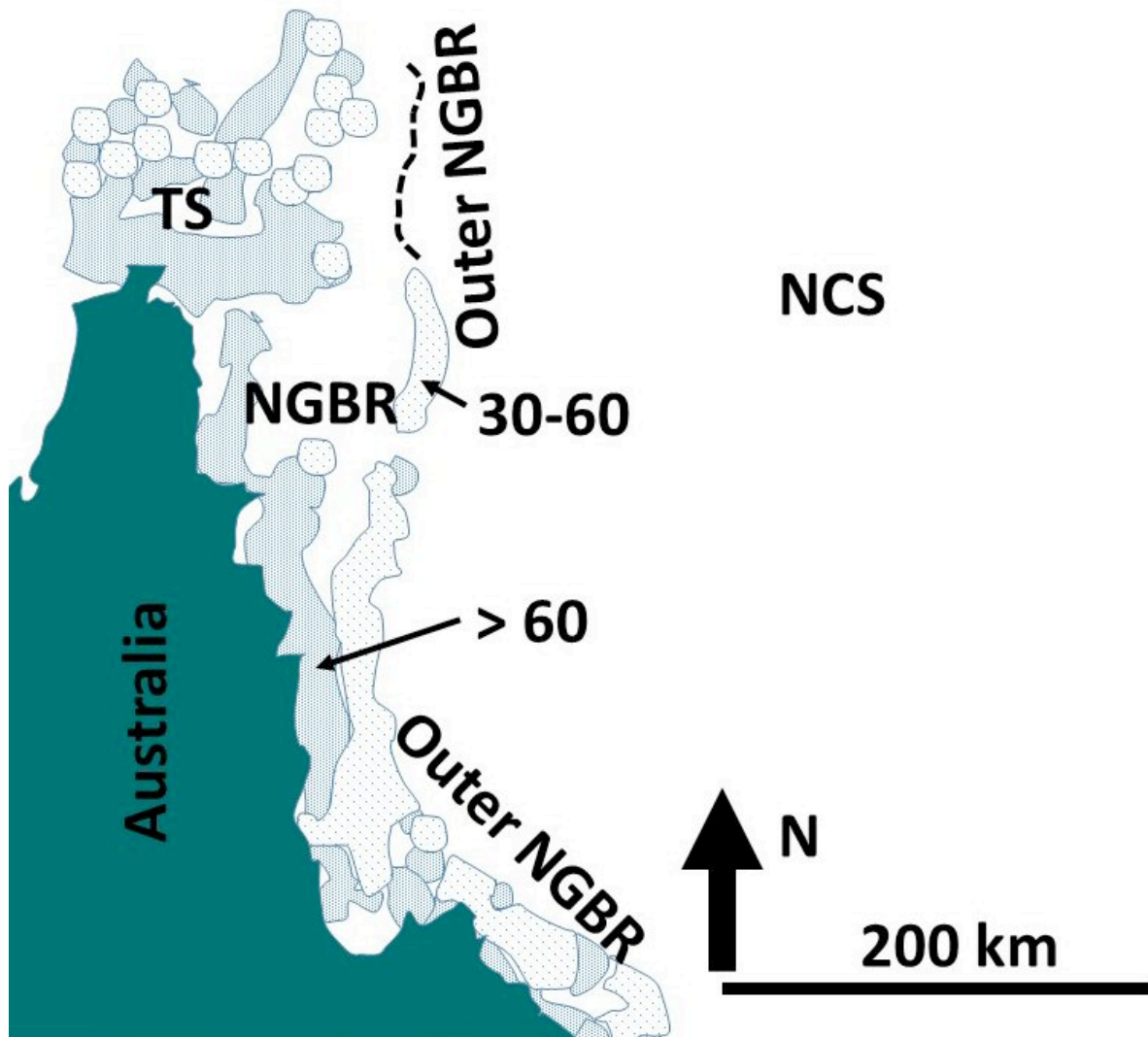


Figure 9: A map of the coral bleaching distribution (in %) in the NGBR and TS following the 2016 ENSO event (redrawn from M. Bode, unp. data).

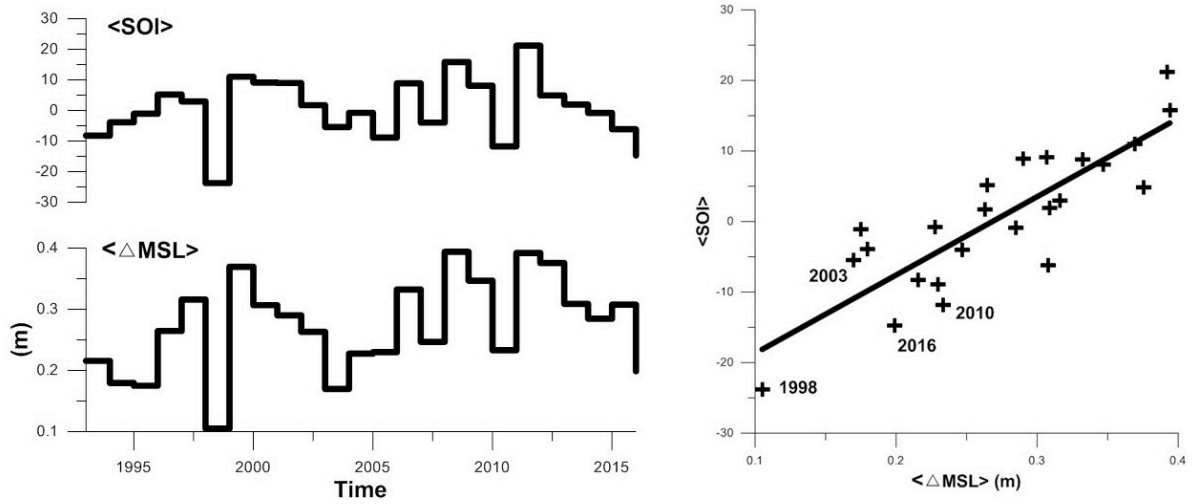


Figure 10: (Left) Time-series plot from 1993 to 2016 of the average SOI ($\langle \text{SOI} \rangle$) and the average difference in mean sea level across Torres Strait ΔMSL ($\langle \Delta \text{MSL} \rangle$), both averaged from January 1 to March 31 in each year. (Right) A scatter plot of $\langle \text{SOI} \rangle$ versus $\langle \Delta \text{MSL} \rangle$ highlighting the 1998, 2003, 2010 and 2016 summer ENSO events.